




Article

Effect of ZnO Addition and of Alpha Particle Irradiation on Various Properties of Er³⁺, Yb³⁺ Doped Phosphate Glasses

Arun Poudel ¹, Iuliia Dmitrieva ¹, Regina Gumenyuk ¹, Laura Mihai ² , Dan Sporea ², Ofelia Mureşan ³, Ion Rusen ³, Teemu Hakkarainen ¹, Nadia G. Boetti ⁴ , Tapio Niemi ¹ and Laetitia Petit ^{1,*} 

¹ Laboratory of Photonics, Tampere University of Technology, Korkeakoulunkatu 3, 33720 Tampere, Finland; poudelarun1985@gmail.com (A.P.); iuliia.dmitrieva@student.tut.fi (I.D.); regina.gumenyuk@tut.fi (R.G.); teemu.hakkarainen@tut.fi (T.H.); tapio.k.niemi@tut.fi (T.N.)

² National Institute for Laser, Plasma and Radiation Physics, Center for Advanced Laser Technologies, RO-077125 Măgurele, Romania; laura.mihai@inflpr.ro (L.M.); dan.sporea@inflpr.ro (D.S.)

³ “Horia Hulubei” National Institute of Physics and Nuclear Engineering, Măgurele RO-077125, Romania; ofelia@nipne.ro (O.M.); vata@nipne.ro (I.R.)

⁴ Istituto Superiore Mario Boella, Via P. C. Boggio 61, 10138 Torino, Italy; boetti@ismb.it

* Correspondence: laetitia.petit@tut.fi; Tel.: +358-50-447-8481

Received: 6 October 2017; Accepted: 20 October 2017; Published: 24 October 2017

Featured Application: The newly developed Er³⁺, Yb³⁺ doped phosphate glasses presented in this paper could find many different applications in space, telecommunications, LIDAR, spectroscopy and bioimaging, just to cite a few.

Abstract: New Er³⁺, Yb³⁺ codoped phosphate glasses with the (98-x) (0.50P₂O₅-0.40SrO-0.10Na₂O)-0.5Er₂O₃-1.5Yb₂O₃-xZnO (in mol %) composition were prepared by melting process with up to 10 mol % of ZnO. The impact of the changes in the glass composition on the thermal, optical, structural properties was investigated. Using IR and Raman spectroscopies, we confirmed that the addition of ZnO up to 10 mol % leads to a depolymerization of the network without having a significant impact on the Er³⁺ and Yb³⁺ sites. We also discuss the effect of alpha particles irradiation. The glass with 2.5 mol % of ZnO was irradiated with 3 MeV alpha particles and a total fluence of 10¹² α/cm². After irradiation, this glass exhibits surface expansion (measured at ~200 nm, 1.5 months after the irradiation) and an increase in the surface roughness. The alpha particles irradiation is suspected to lead to changes in the spectroscopic properties of the glass. Finally, the photo-response of the glass was found to be reversible.

Keywords: phosphate glasses; Yb³⁺ and Er³⁺ codoping; spectroscopic properties; IR and Raman spectroscopies; alpha particle irradiation

1. Introduction

Erbium-doped glasses are of crucial importance due to the generation of light at 1520–1570 nm, which corresponds to the intra-4f transition of Er³⁺ from ⁴I_{13/2} to ⁴I_{15/2} [1]. There has been a constant need for improving the performance of such glasses, which could be achieved by developing new glass materials. Oxide glasses are known to be promising hosts for obtaining efficient luminescence from rare-earth (RE) ions [2]. Especially, Er³⁺ doped phosphate glasses have been intensively studied for many years, as they are easy to process and they also possess good thermal stability and excellent optical characteristics, such as high transparency in the UV-Visible-Near Infrared (UV-Vis-NIR)

region [3]. Additionally, they can incorporate a high amount of Er^{3+} ions (as opposed to silicate glasses) without Er–Er clustering. It is well known that the local environment around the RE ions has a significant impact on the optical and spectroscopic properties of glasses [4]. In our recent study [5], we investigated the changes in the thermal, structural and luminescence properties of Er^{3+} doped phosphate glasses induced by the addition of Al_2O_3 , TiO_2 and ZnO in low amount (1.5 mol %). We found that the addition of Al_2O_3 and TiO_2 has only a slight impact on the density, glass structure and spectroscopic (absorption and emission) properties of the glasses whereas the addition of ZnO increases the intensity of the emission at 1540 nm probably due to the depolymerization of the phosphate network. Therefore, we report here new findings on the preparation of the Er^{3+} doped phosphate glasses with larger amount of ZnO to confirm the role of Zn in the glass network and, more importantly, its impact on the site of Er^{3+} ions.

Er^{3+} doped glasses could find applications in telecommunications, LIDAR (Light Detection and Ranging), spectroscopy and bioimaging, just to cite a few. Recently, such materials were also found to be useful for optical inter-satellite links and other applications, such as amplifiers for highly distributed data networks and broadband super luminescent sources for fiber gyroscopes [6]. It was found that rare-earth doped fibers are more sensitive to irradiation than undoped optical fibers due to the formation of defects or color centers in the glass matrix, which lead to changes in the spectroscopic properties of the glasses and in the fiber losses [7]. The factors affecting the radiation-induced loss on doped fibers are: (i) the type of ionizing radiation; (ii) total absorbed dose; (iii) dose rate; (iv) rare-earth dopant concentrations; and (v) the fabrication parameters as reported in [8]. Therefore, when developing new Er^{3+} doped glasses, the radiation effect in these glasses should be investigated in order to develop new radiation-resistant fibers suitable for space applications and nuclear environments. Our group in the National Institute for Laser, Plasma and Radiation Physics (Romania) has been running for several years, tests of ionizing radiation effects on optoelectronic materials components and device, optical fibers and optical fiber sensors, especially under gamma-ray, proton, electron beam, neutron, alpha particles irradiation, which are of interest for space applications or the operation of nuclear installations (nuclear power plants, nuclear waste repositories). Radiation hardening tests are of interest in relation to specific space missions, as ionizing radiation originating outside of Earth's atmosphere is constituted by 87% of protons, 12% of alpha particles and 1% of heavy elements. Recently, we reported, for the first time, a comprehensive study on alpha particle irradiation effects on four mid-IR materials [9] and gamma-ray-induced changes in Bi/Er co-doped optical fibers [10]. Our investigations brought several novelties to the field of material research operating in harsh environments (i.e., ionizing radiation) and in the use of THz spectroscopy and imaging in the evaluation of irradiated optical materials. Surprisingly, very few studies on irradiation of phosphate glass can be found. Here, we bring additional knowledge on the alpha particles irradiation effects on Er^{3+} , Yb^{3+} co-doped phosphate glasses.

Therefore, the aim of this work is to process new phosphate glasses with large amount of ZnO (up to 10 mol%) and understand the role of the changes in the glass composition on the thermal, structural and luminescence properties of the newly developed glasses. We also investigate the impact of alpha particles radiation on the surface and luminescence properties of the glass prepared with 2.5 mol % of ZnO . We show that the alpha particles radiation-induced change is a reversible process.

2. Materials and Methods

Different glasses with the system $(98-x) (0.50\text{P}_2\text{O}_5-0.40\text{SrO}-0.10\text{Na}_2\text{O}) -0.5\text{Er}_2\text{O}_3-1.5\text{Yb}_2\text{O}_3-x\text{ZnO}$ (in mol %) with $x = 0, 2.5, 5$ and 10 (labeled Ref., 2.5Zn, 5Zn, 10Zn) were prepared using a standard melting method in air. NaPO_3 , SrCO_3 , $(\text{NH}_4)_2\text{HPO}_4$, Yb_2O_3 , Er_2O_3 and ZnO were used as raw materials for the batch preparation. $\text{Sr}(\text{PO}_3)_2$ was separately prepared from the mixture of SrCO_3 and $(\text{NH}_4)_2\text{HPO}_4$ using slow heating rate up to 850°C . The 10 g batches were mixed in a mortar, and melted in platinum crucible for 30 min between 1150°C to 1525°C , depending on the glass composition. To ensure the homogeneity of the molten glass, the glass melt was mixed before

quenching. After quenching, the glasses were annealed at 40 °C below their respective glass transition temperature for 5 h to release the stress from the quench. Finally, the glass samples were polished and also crushed into powder. A scanning electron microscope (Carl Zeiss Crossbeam 540) equipped with Oxford Instruments X-MaxN 80 EDS detector was used to check the composition of the glasses and within the accuracy of the analysis (± 1.5 mol %), the composition of all the glasses was found to be in agreement with the nominal one.

The glass transition temperature (T_g) and crystallization temperature (T_p) were measured by differential thermal analysis (DTA) using a Netzsch JUPITER F1 instrument. The measurement was carried out in a Pt crucible at a heating rate of 10 °C/min. T_g was determined as the inflection point of the endotherm obtained by taking the first derivative of the DTA curve, while T_p was taken as the maximum peak of the exotherm. The onset of the crystallization peak, T_x , was also measured. All measurements were performed with an error of ± 3 °C.

The density of the glasses was measured using Archimedes' method with an accuracy of ± 0.02 g/cm³, using ethanol as immersion liquid.

The absorption spectra of the bulk glasses were measured using UV-Vis-NIR spectrophotometer (UV-360 Plus, Shimadzu) from 200 to 1750 nm with the resolution of 0.5 nm. The absorption cross-section $\sigma_{abs}(\lambda)$ is calculated using Equation (1).

$$\sigma_{Abs}(\lambda) = \frac{2.303}{NL} \log\left(\frac{I_0}{I}\right) \quad (1)$$

where $\log(I_0/I)$ is the absorbance, L is the thickness of the sample (in cm) and N is the concentration of rare-earth ions (ions/cm³). The concentration of Er³⁺ ions was calculated from the measured glasses density. The accuracy of absorption cross-section measurement was $\pm 10\%$.

The IR spectra were measured using a 'Perkin Elmer Spectrum one FTIR (Fourier-transform infrared spectroscopy) spectrometer' in Attenuated Total Reflectance (ATR) mode in mid infrared region 600–1400 cm^{−1}. The resolution used was 2 cm^{−1} and the spectra were obtained from the accumulation of 8 scans.

The Raman spectra of the samples were measured using Thermo Scientific™ DXR™ 2xi Raman imaging microscope. The wavelength of the laser was 532 nm and the power at the sample was 2.0 mW. The exposure time was 0.2 s per pixel and data was averaged four times.

The emission spectra in the 1400–1700 nm range were measured on sample crushed into powder with a Jobin Yvon iHR320 spectrometer equipped with a Hamamatsu P4631-02 detector and a filter (Thorlabs FEL 1500). Emission spectra were obtained at room temperature using an excitation monochromatic light at 976 nm, emitted by a single-mode fiber pigtailed laser diode (CM962UF76P-10R, Oclaro). The fluorescence lifetime of Er³⁺:⁴I_{13/2} energy level was obtained by exciting the samples with laser pulses of the 976 nm laser diode, recording the signal using a digital oscilloscope (Tektronix TDS350) and fitting the decay traces by single exponential. Estimated error of the measurement was ± 0.20 ms. The detector used for this measurement was a Thorlabs PDA10CS-EC.

The glass with $x = 2.5$ was irradiated with 3 MeV alpha particles from the U-120 Cyclotron accelerator. The beam current was 3 nA and the total fluence was 10^{12} α/cm². The UV-Vis-NIR transmittance spectra were measured using an Ocean Optics QE65000 spectrometer with operation between 200 and 900 nm. The detector is thermoelectric-cooled and has a CCD (charge coupled device) array from Hamamatsu with 1044 × 64 elements and a dynamic range of 40,000:1 for a single integration time. The reflectance in 0.06–2 THz range spectra were obtained using TPS Spectra 3000 THz spectrometer from TeraView. The resulting photo-modified surface profile was then analyzed using Wyko NT1100 optical profiling system to assess photo-induced surface modification. The surface roughness data such as Ra (arithmetical mean deviation of the assessed profile), Rq (root mean squared), Rz (average distance between the highest peak and lowest valley) and Rt (Maximum Height of the Profile) were determined. After irradiation, the micro-photoluminescence (PL) was measured at the surface of the glasses at room temperature using the 532 nm line of a continuous-wave Nd:YAG

laser for excitation. The excitation laser beam was focused on the sample with a 40X magnifying high-numerical aperture (NA) objective. The photoluminescence signal was collected with the same objective and detected with a TE-cooled InGaAs array camera attached to a 750 mm spectrometer. The spatial resolution of the micro-PL setup was 1 μm .

3. Results and Discussion

Phosphate glasses were prepared using standard melting method in air and with 0.5 mol % Er_2O_3 and 1.5 mol % Yb_2O_3 . Different concentrations of ZnO (x) were added in the glass within the glass system $(98-x) (0.50\text{P}_2\text{O}_5-0.40\text{SrO}-0.10\text{Na}_2\text{O}) -0.5\text{Er}_2\text{O}_3-1.5\text{Yb}_2\text{O}_3-x\text{ZnO}$ (in mol %). The thermal and physical properties of the investigated glasses are listed in Table 1.

Table 1. Physical and thermal properties of the glasses.

Glass Label	x	ρ ($\text{g}\cdot\text{cm}^{-3}$) $\pm 0.02 \text{ g}\cdot\text{cm}^{-3}$	T_g ($^\circ\text{C}$) $\pm 3 \text{ }^\circ\text{C}$	T_x ($^\circ\text{C}$) $\pm 3 \text{ }^\circ\text{C}$	T_p ($^\circ\text{C}$) $\pm 3 \text{ }^\circ\text{C}$	ΔT ($^\circ\text{C}$) $\pm 6 \text{ }^\circ\text{C}$
REF	0	3.21	462	580	593	118
2.5 Zn	2.5	3.23	466	576	596	110
5 Zn	5	3.26	445	560	577	115
10 Zn	10	3.32	444	549	570	105

The glass density increases with an increase in x due to the partial replacement of P_2O_5 , Na_2O and SrO by the heavier Zn atoms in glass network. The decrease in T_g with an increase in ZnO content (x) could indicate that Zn acts as a network modifier. Similar changes in the physical and thermal properties induced by ZnO were reported in [11]. Also shown in the table is ΔT , the temperature difference between T_x and T_g , which is an indicator of the glass resistance to crystallization. No real impact of the addition of ZnO can be noticed on the thermal stability of the glasses.

In order to understand better the changes in the physical and thermal properties of the glasses induced by the addition of ZnO, the IR and Raman spectra of the glasses were measured and they are presented in Figure 1a,b, respectively.

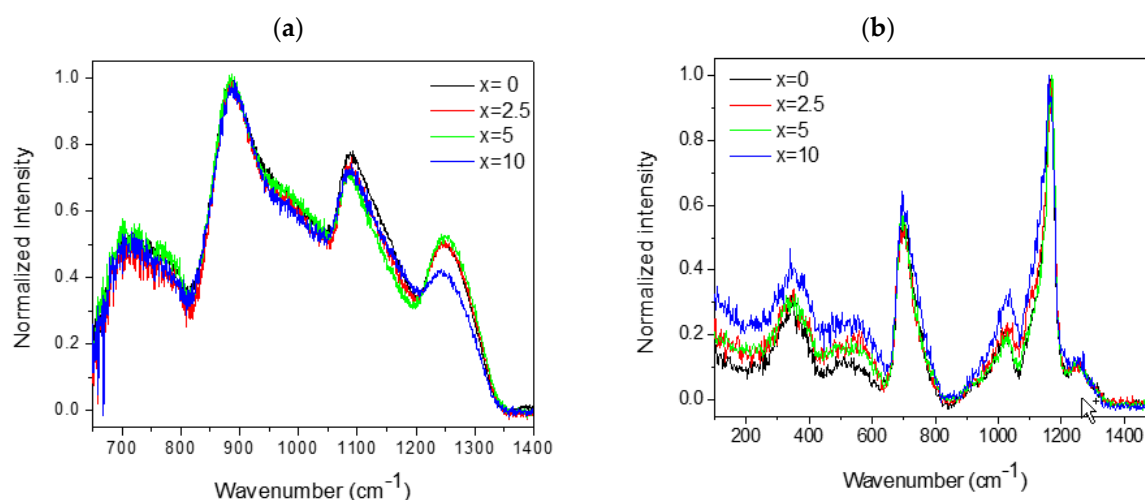


Figure 1. IR (a) and Raman (b) spectra of the investigated glasses.

The IR spectra in Figure 1a are normalized to the main band at 880 cm^{-1} , thus all the discussed intensity changes are expressed relatively to the main band. The spectra exhibit a broad band between 650 and 800 cm^{-1} , three absorption bands located at around 885 , 1085 and 1260 cm^{-1} , and a shoulder at 980 cm^{-1} . They are similar to the IR spectra reported in [5]. The broad band between 650 and 800 cm^{-1}

can be related to symmetric vibrational modes $\nu_{\text{sym}}(\text{P}-\text{O}-\text{P})$ of Q^2 units [12]. The strong absorption band at 885 cm^{-1} is due to asymmetric stretching vibrational modes $\nu_{\text{as}}(\text{P}-\text{O}-\text{P})$ in Q^2 units [12,13]. The shoulder appearing in the $930\text{--}1010\text{ cm}^{-1}$ range can be associated to rings-type [14]. The shoulder centered at 980 cm^{-1} and the band at 1085 cm^{-1} are due to symmetric and asymmetric stretching vibrations of Q^1 units, respectively [15]. The band at 1085 cm^{-1} can be attributed to an overlap between Q^1 units and Q^2 units in metaphosphate [15]. The shoulder at 1160 cm^{-1} and the band at 1250 cm^{-1} are mainly due to symmetric and asymmetric vibrations of PO_2^- in Q^2 units respectively [16]. As seen in [5], no bands can be seen at wavenumber larger than 1300 cm^{-1} , where the $\nu(\text{P}=\text{O})$ of Q^3 groups typically appear. The progressive addition of ZnO leads to a decrease in intensity of the bands at 1085 and 1250 cm^{-1} and also of the shoulders in the $930\text{--}1010\text{ cm}^{-1}$ range compared to the main band. A shift of all the bands towards smaller wavenumbers can also be observed, which is a clear sign of changes in the strength of the chemical bonds in the glass network.

The Raman spectra of glasses in Figure 1b are normalized to the band at $\sim 1170\text{ cm}^{-1}$, thus all the discussed intensity changes are expressed relatively to this main peak. The Raman spectra of the glasses exhibit bands at 300 , 500 , ~ 700 , 1170 and 1280 cm^{-1} and several bands between 800 and 1110 cm^{-1} . As for the IR spectra, those Raman spectra are similar to those reported in [5]. The band at 300 cm^{-1} can be attributed to ZnO_4 units and the bands in the $400\text{--}600\text{ cm}^{-1}$ range can be related to bend mode of phosphate polyhedral and to Zn-O vibration [17]. The band centered at 700 cm^{-1} can be related to the symmetric stretching of bridging $\nu_{\text{sym}}(\text{P}-\text{O}-\text{P})$ of Q^2 groups and the band at 1020 cm^{-1} to the symmetric stretching $\nu_{\text{sym}}(\text{P}-\text{O})$ of terminal Q^1 groups [12]. The bands at ~ 1170 and 1280 cm^{-1} can be attributed to symmetric and asymmetric stretching of non-bridging $\nu(\text{PO}_2^-)$ of Q^2 groups, respectively [18]. As seen in [5], there is no evidence of Q^3 units, usually appearing in wavenumber larger than 1300 cm^{-1} , although the concentration of ZnO was increased up to $10\text{ mol } \%$. With the addition of ZnO, the bands in the $200\text{--}1100\text{ cm}^{-1}$ range increase in intensity compared to that of the main band.

Before discussing the IR and Raman spectra, it is crucial to recapitulate the structure of a phosphate glass. As explained in [11], in ultraphosphate glasses ($[\text{P}_2\text{O}_5] > 50\text{ mol } \%$), the structural units are Q^3 and Q^2 tetrahedra, the Q^3 units forming the 3D network, while the Q^2 units assist the chain formation. With a decrease in P_2O_5 content, the structure of the glass becomes metaphosphate formed by Q^2 units with chains of $(\text{P}-\text{O}-\text{P})$ -bridges and rings. Further reduction in P_2O_5 content leads to the formation of polyphosphate glasses formed by shorter chains of Q^2 , which are terminated by Q^1 units. Although the ZnO content was increased up to $10\text{ mol } \%$, the IR and Raman spectra still clearly indicate the presence of a metaphosphate structure. The presence of the Raman bands at $\sim 700\text{ cm}^{-1}$ indicates that the chains are present with different lengths. We confirm our former assumption in [5] that up to $10\text{ mol } \%$, ZnO enters as a modifier leading to a depolymerization of the network and to a less cross-linked network, as seen by an increase of the Q^1 units at the expense of the expense of the Q^2 units. This is in agreement with the decrease in the T_g seen with an increase in x (Table 1).

The absorption spectra and the normalized emission spectra of the investigated glasses are shown in Figure 2a,b, respectively.

The absorption spectra exhibit several bands, which are characteristics of the Er^{3+} ions $4f\text{--}4f$ transitions from the ground state to various excited levels [19]. The absorption band at 975 nm can be also related to the Yb^{3+} $4f\text{--}4f$ ($^2\text{F}_{7/2} \rightarrow ^2\text{F}_{5/2}$) transition, which overlaps with the weak absorption band due to the Er^{3+} $4f\text{--}4f$ ($^4\text{I}_{15/2} \rightarrow ^4\text{I}_{11/2}$) transition. An increase in x leads to a shift of the band gap to longer wavelength probably due to the depolymerization of the phosphate as explained in [5]. The absorption cross-section at 975 nm and $1.5\text{ }\mu\text{m}$ were calculated from the absorption coefficient using Equation (1) and are presented in Table 2.

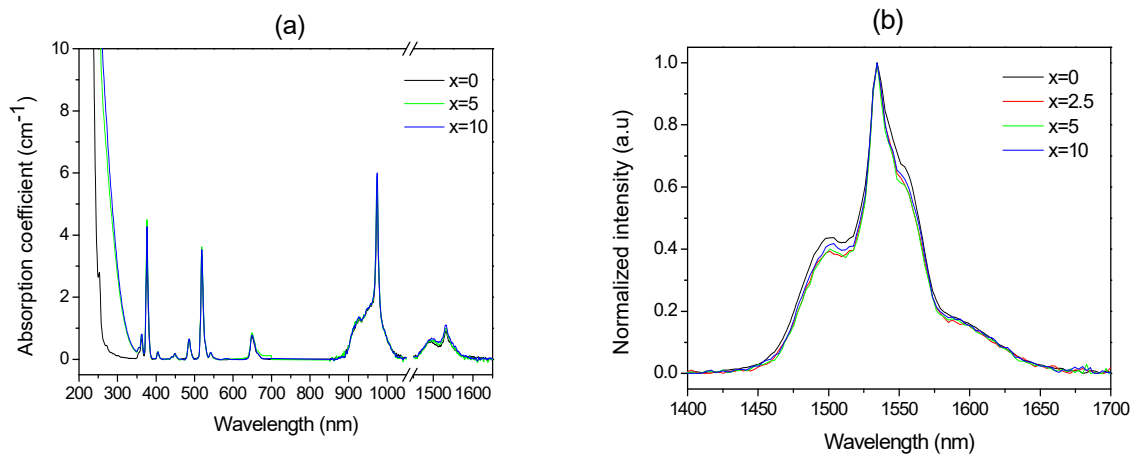


Figure 2. UV-Vis-NIR absorption (a) and normalized emission (b) spectra of the investigated glasses. The emission spectra were obtained using a 976 nm excitation.

Table 2. Optical and luminescence properties of the glasses.

Glass Label	x	Er ³⁺ Ions·cm ^{−3} (10 ²⁰) ±5%	Yb ³⁺ Ions·cm ^{−3} (10 ²⁰) ±5%	σ _{Abs} at 980 nm (10 ^{−21} cm ²) ±10%	σ _{Abs} at 1550 nm (10 ^{−21} cm ²) ±10%	Er ³⁺ : ⁴ I _{13/2} τ (ms) ±0.20 ms
REF	0	1.58	4.75	8.30	5.79	3.47
2.5 Zn	2.5	1.56	4.68	8.28	6.32	3.19
5 Zn	5	1.60	4.81	9.12	6.23	2.98
10 Zn	10	1.66	4.97	9.06	6.63	3.27

Within the error of the measurement, the absorption cross-section at 1.5 μm are similar to those reported in [5]. However, the absorption cross-section at 975 nm of the investigated glasses are larger than those reported in [5] due to the Yb³⁺ codoping. We confirm the absence of variation in the absorption cross-section at 975 nm and at 1.5 μm with an increase in x up to 10 mol %, indicating that the sites of the Er³⁺ and Yb³⁺ ions are not strongly affected by the change in the glass composition. Although the progressive addition of ZnO has a noticeable impact on the structure, we confirm that up to 10 mol %, Zn ions do not enter in the second coordination shell around the Er³⁺ and Yb³⁺ ions. Therefore, these Er³⁺ and Yb³⁺ ions are thought to be surrounded mainly by P, Na and Sr.

The emission spectra of the glasses were measured using a 975 nm pumping. No noticeable increase in the intensity of emission at 1.5 μm was observed in agreement with the absorption cross-section at 975 nm presented in Table 2. The normalized emission spectra of the prepared glasses under 975 nm excitation wavelength are displayed in Figure 2b. The spectra of the glasses exhibit an emission band, which is typical of Er³⁺ emission (⁴I_{13/2} → ⁴I_{15/2}) in glass, with a bandwidth of 42 nm. An increase in the concentration of ZnO leads to small changes in the shape of the emission band confirming that Er³⁺ and Yb³⁺ ions' sites are not strongly affected by the changes in the glass composition. The lifetime values of Er³⁺:⁴I_{13/2} level in the investigated glasses were measured and are reported in Table 2. Within the accuracy of the measurement, the lifetime values do not depend on x. Surprisingly, it should be pointed out that the lifetime values in the investigated glasses are smaller than those reported in [5].

The glass with x = 2.5 was irradiated using alpha particles. No craters or cracks were formed during the irradiation of the glasses. The alpha particles irradiation leads to the appearance of spot which could be seen with naked eyes and also with a 3D interference microscope as shown in Figure 3a.

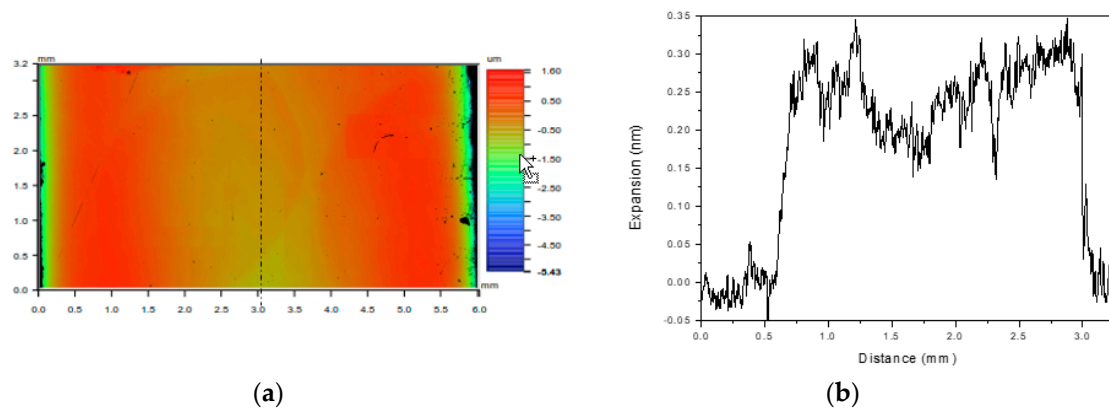


Figure 3. Image of spots at the surface of the glass (a) and its surface profile (b) using Wyko NT1100 optical profiling system.

The spot corresponds to a surface photo-expansion of ~ 200 nm (Figure 3b). As reported in [20], this surface photo-expansion could be attributed to macroscopic and microscopic structural changes in the glass due to defects such as oxygen vacancies, trapped electron and hole centers or to structural deformations. Analysis of the changes in the glass structure using micro-Raman spectroscopy is in progress, and it will be reported separately. Associated with the surface photo-expansion, the surface roughness was found to increase after irradiation as reported in Table 3.

Table 3. Surface roughness parameters of the glass surface measured after (1.5 and 3 months) irradiation and after heat treatment.

	Ra (nm)	Rq (nm)	Rz (nm)	Rt (nm)
Prior to Heat Treatment				
Non-irradiated area	38	46	431	505
Irradiated spot measured 1.5 months after the irradiation	219	250	1470	2640
Irradiated spot measured 3 months after the irradiation	121	154	621	642
After Heat Treatment at 400 °C for 8 h				
Non-irradiated area	66	76	319	336
Former irradiated spot	162	191	897	926

We noticed that the increase in the surface roughness is a reversible process as it decreases progressively over a period of 3 months, although the glass was stored in the dark at room temperature. However, no significant change in the surface expansion could be detected during these 3 months. We found that a heat treatment of the glass at 400 °C for 8 h, which corresponds to the annealing step in the glass melting process, is sufficient to erase the spot created by the irradiation but has no significant impact on the surface roughness. Further optimization of the heat treatment post irradiation is in progress to photo-bleach the irradiated glass.

The UV-Vis-NIR transmittance and the reflectance in THz range, measured prior to and right after irradiation, are presented in Figure 4a,b, respectively.

The transmittance in UV-Vis-NIR range decreases after irradiation, which is in agreement with the appearance of the visible spot. Similar decreases in the transmission after alpha particles irradiation were reported in different materials such as CaF_2 , Al_2O_3 or ZnSe due to the formation of color centers [9]. The absorption coefficients in the visible wavelength range of the Er^{3+} 4f-4f transitions also decrease after irradiation indicating that the irradiation has a significant impact on the Er^{3+} ions sites. As seen in Figure 4b, the alpha particle irradiation also produces a change of the THz frequency signal: no shift in the maximum was observed, but as seen in the case of Al_2O_3 and ZnSe , only a decrease

of the amplitude can be noticed after irradiation. This can be related to the formation of defects or to structural deformations occurring during the irradiation.

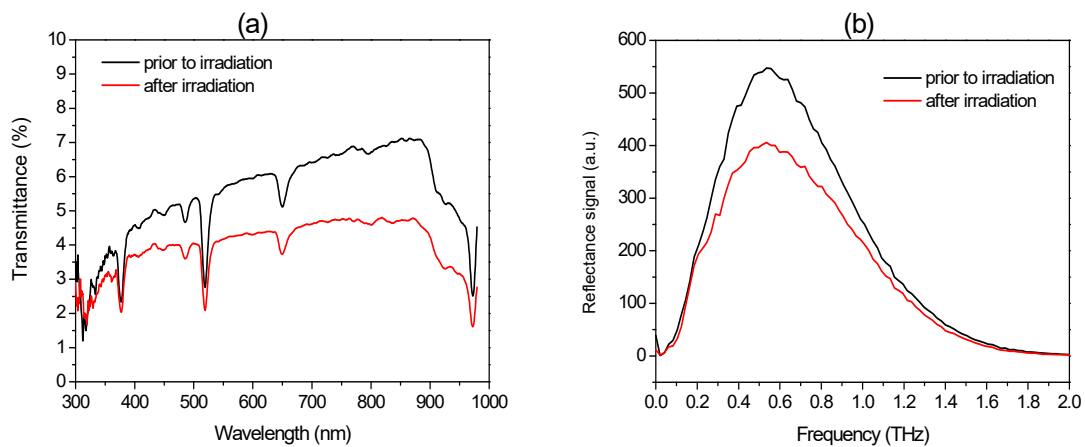


Figure 4. UV-Vis-NIR transmittance (a) and reflectance in THz range (b) spectra of the glass with $x = 2.5$ prior to and after irradiation.

The micro-PL spectrum of the irradiated spot was measured 3 months after the irradiation. The spectrum was compared to the micro-PL spectrum collected from a non-irradiated area. The spectra are shown in Figure 5.

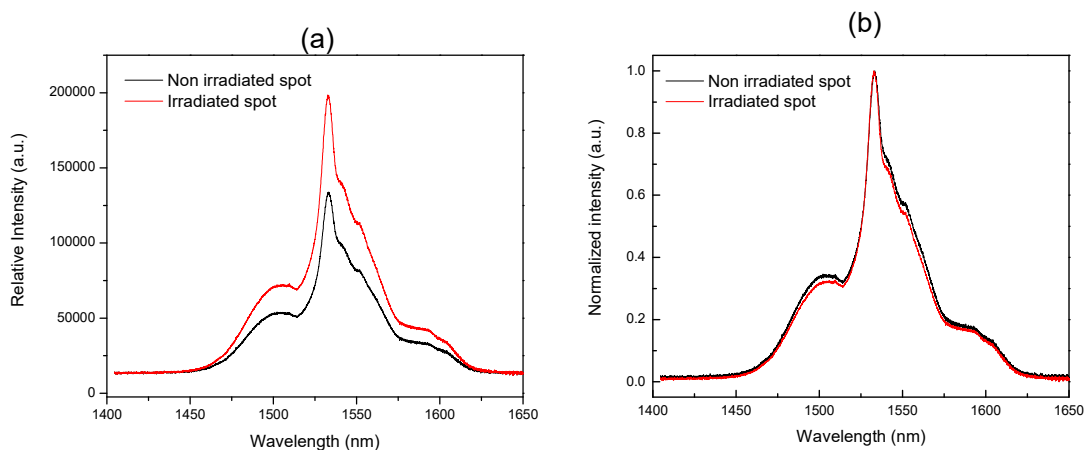


Figure 5. Emission (a) and normalized emission (b) spectra measured in non-irradiated and irradiated spots.

The 3-month-old irradiated spot exhibits a slightly larger emission than the non-irradiated area of the glass. As seen in Figure 5b, the irradiation might also lead to small changes in the site of Er^{3+} ions. As the irradiation took place in vacuum, hence poorer heat dissipation occurred in these samples produces local thermal stress. It is possible to think that the irradiation of the glass reduces the amount of OH groups, which are known to diminish the emission intensity by non-radiative phenomena [21]. Additional irradiation experiments using different doses are in progress to confirm the impact of the irradiation on the structure and luminescence properties of the glass.

4. Conclusions

Glasses with the system (98-x) (0.50P₂O₅-0.40SrO-0.10Na₂O)-0.5Er₂O₃-1.5Yb₂O₃-xZnO (in mol %) were prepared using melt-quenching technique. The physical, thermal, structural, optical and spectroscopic properties of the glasses were measured. Using IR and Raman spectroscopies,

the structure of the glass is suspected to be a metaphosphate structure with Q^2 and Q^1 network units. We confirm that Zn ions act as network modifiers and lead to a depolymerization of phosphate network in agreement with the decrease in T_g . While the progressive addition of ZnO in the phosphate network has an impact on the structure of the glass, Zn ions have no significant impact on the sites of the Er^{3+} and Yb^{3+} ions. Er^{3+} and Yb^{3+} ions are thought to be surrounded mainly by P, Na and Sr.

In this paper, we also discuss the effect of the alpha particles irradiation on the surface, optical and micro-luminescence properties of the glass with $x = 2.5$. We showed that this glass is sensitive to alpha particles irradiation and exhibits a surface photo-expansion of ~ 200 nm (measured 1.5 month after the irradiation). The irradiation also increased the surface roughness and is suspected to also increase the emission at ~ 1.5 μm due to changes in the coordination sites of Er^{3+} and/or to changes in the OH content. The photo-response of the glass was found to be reversible. Three months after the irradiation, a noticeable reduction in the surface photo-expansion was observed although the glass was stored in the dark at room temperature.

In summary, our investigation brought additional novelties to the field of material research operating in harsh environments (i.e., ionizing radiation), clearly showing the need to further investigate the radiation effect of glasses with different compositions in order to develop new photo-resistant glasses for space application.

Acknowledgments: This work was supported by the Academy of Finland through the Competitive Funding to Strengthen University Research Profiles program (310359), academy project (308558) and Academy of Finland Postdoctoral research project (285170). The Romanian authors acknowledge the financial support of the Romanian Executive Agency for Higher Education, Research, Development and Innovation Funding (UEFISCDI), under the contract 24 PED/2017, project “Photonics devices under extreme operating conditions”—PHOENIX. The cooperation was run under the COST Action MP1401 “Advanced Fibre Laser and Coherent Source as Tools for Society, Manufacturing and Lifescience”.

Author Contributions: T.N. and L.P. conceived and designed the experiments; A.P. performed the experiments; ID performed the surface profile measurement of the irradiated samples; R.G. and N.G.B. were in charge of the measurement of the luminescence (emission and lifetime) properties; the teams from Romania performed the irradiation of the glasses and THz measurements of the irradiated samples. L.P. wrote the paper, which was reviewed and approved by all co-authors.

Conflicts of Interest: The founding sponsors had no role in the design of the study; in the collection, analyses, or interpretation of data; in the writing of the manuscript, and in the decision to publish the results.

References

- Miniscalco, W.J. Erbium-doped glasses for fiber amplifiers at 1500 nm. *J. Lightwave Technol.* **1991**, *9*, 234–250. [[CrossRef](#)]
- Martucci, A.; Chiasera, A.M.; Montagna, M. Ferrari, Erbium-doped GeO_2 – TiO_2 sol–gel waveguides. *J. Non-Cryst. Solids* **2003**, *322*, 295–299. [[CrossRef](#)]
- Jiang, S.; Myers, M.; Peyghambarian, N. Er^{3+} doped phosphate glasses and lasers. *J. Non Cryst. Solids* **1998**, *239*, 143–148. [[CrossRef](#)]
- Oppo, C.I.; Corpino, R.; Ricci, P.C.; Paul, M.C.; Das, S.; Pal, M.; Bhadra, S.K.; Yoo, S.; Kalita, M.P.; Boyland, A.J.; et al. Incorporation of Yb^{3+} ions in multicomponent phase-separated fibre glass preforms. *Opt. Mater.* **2012**, *34*, 660–664. [[CrossRef](#)]
- Lopez-Iscoa, P.; Petit, L.; Massera, J.; Janner, D.; Boetti, N.G.; Pugliese, D.; Fiorilli, S.; Novara, C.; Giorgis, F.; Milanese, D. Effect of the addition of Al_2O_3 , TiO_2 and ZnO on the thermal, structural and luminescence properties of Er^{3+} -doped phosphate glasses. *J. Non Cryst. Solids* **2017**, *460*, 161–168. [[CrossRef](#)]
- Rose, T.S.; Gunn, D.; Valley, G.C. Gamma and proton radiation effects in erbium-doped fiber amplifiers: Active and passive measurements. *J. Lightwave Technol.* **2001**, *19*, 1918–1923. [[CrossRef](#)]
- Tortech, B.; Ouerdane, Y.; Girard, S.; Meunier, J.P.; Boukenter, A.; Robin, T.; Cadier, B.; Crochet, P. Radiation effects on Yb- and Er/Yb-doped optical fibers: A micro-luminescence study. *J. Non Cryst. Solids* **2009**, *355*, 1085–1088. [[CrossRef](#)]
- Williams, G.M.; Putnam, M.A.; Askins, C.G.; Gingerich, M.E.; Friebele, E.J. Radiation effects in erbium-doped optical fibres. *Electron. Lett.* **1992**, *28*, 1816–1818. [[CrossRef](#)]

9. Sporea, D.; Mihai, L.; Sporea, A.; Văță, I. Optical and THz investigations of mid-IR materials exposed to alpha particle irradiation. *Sci. Rep.* **2017**, *7*, 40209. [[CrossRef](#)] [[PubMed](#)]
10. Sporea, D.; Mihai, L.; Neguț, D.; Luo, Y.; Yan, B.; Ding, M.; Wei, S.; Peng, G.-D. γ irradiation induced effects on bismuth active centres and related photoluminescence properties of Bi/Er co-doped optical fibres. *Sci. Rep.* **2017**, *6*, 29827. [[CrossRef](#)] [[PubMed](#)]
11. Schwarz, J.; Ticha, H.; Tichy, H.; Mertens, R. Physical Properties PbO-ZnO-P₂O₅ glasses I. Infrared and Raman spectra. *J. Optoelectron. Adv. Mater.* **2004**, *6*, 737–746.
12. Konidakis, I.; Varsamis, C.-P.E.; Kamitsos, E.I.; Möncke, D.; Ehrt, D. Structure and properties of mixed strontium-manganese metaphosphate glasses. *J. Phys. Chem. C* **2010**, *114*, 9125–9138. [[CrossRef](#)]
13. Moustafa, Y.M.; El-Egili, K. Infrared spectra of sodium phosphate glasses. *J. Non Cryst. Solids* **1998**, *240*, 144–153. [[CrossRef](#)]
14. Wilder, J.A.; Shelby, J.E. Property variation in alkali alkaline-earth metaphosphate glasses. *J. Am. Ceram. Soc.* **1984**, *67*, 438–444. [[CrossRef](#)]
15. Bruni, S.; Cariati, F.; Narducci, D. Infrared specular reflection spectra of copper-zinc phosphate glasses. *Vib. Spectrosc.* **1994**, *7*, 169–173. [[CrossRef](#)]
16. Meyer, K. Characterization of the structure of binary zinc ultraphosphate glasses by infrared and Raman spectroscopy. *J. Non Cryst. Solids* **1997**, *209*, 227–239. [[CrossRef](#)]
17. Liu, H.S.; Chin, T.S.; Yung, S.W. FTIR and XPS studies of low melting PbO-ZnO-P₂O₅ glasses. *Mater. Chem. Phys.* **1997**, *50*, 1–10. [[CrossRef](#)]
18. Karakassides, M.A.; Saranti, A.; Koutselas, I. Preparation and structural study of binary phosphate glasses with high calcium and/or magnesium content. *J. Non Cryst. Solids* **2004**, *347*, 69–79. [[CrossRef](#)]
19. Barrière, A.S.; Raoux, S.; Garcia, A.; L'Haridon, H.; Lambert, B.; Moutonnet, D. Intra-4f-shell transitions at room temperature of Er³⁺ ions in Ca_{1-x} Er_x F_{2+x} thin films grown on Si(100). *J. Appl. Phys.* **1994**, *75*, 1133–1137. [[CrossRef](#)]
20. Yliniemi, S.; Honkanen, S.; Ianoul, A.; Laronche, A.; Albert, J. Photosensitivity and volume gratings in phosphate glasses for rare-earth-doped ion-exchanged optical waveguide lasers. *J. Opt. Soc. Am. B* **2006**, *23*, 2470–2478. [[CrossRef](#)]
21. Yan, Y.; Faber, A.J.; de Waal, H. Luminescence quenching by OH groups in highly Er-doped phosphate glasses. *J. Non Cryst. Solids* **1995**, *181*, 283–290. [[CrossRef](#)]

